

Top Launch 3rd Harmonic X-mode Electron Cyclotron Heating in the TCV Tokamak

S. Alberti, L. Porte, G. Arnoux, T.P. Goodman, M.A. Henderson, J.P. Hogge,
E. Nelson-Melby

*Centre de Recherches en Physique des Plasmas,
Association EURATOM-Confédération Suisse,
EPFL, 1015 Lausanne, Switzerland.*

Introduction

Additional heating in TCV tokamak has been recently upgraded to a total of 4.5 MW of installed ECH power with 3MW 2nd harmonic ECH-ECCD at 82.7 GHz and 1.5 MW 3rd harmonic ECH at 118 GHz. The additional power at the 3rd harmonic allows the electron density range of ECH heated plasmas to be extended to $1 \cdot 10^{20} \text{ m}^{-3}$. Access to these higher densities with additional heating will considerably extend the parameter range of confinement and transport already studied in TCV. It will also permit achievement of H-modes at power levels significantly exceeding the L-H transition power thus allowing the full shape flexibility of TCV to be used in studying the high confinement, ELMing regime.

The choice of the top-launch scheme results as a compromise between heating of high density plasmas and the maximisation of single-pass absorption in ohmically heated target plasmas. The resonance layer is approximately a vertical surface on the high field side of the cold resonance and maximum absorption is obtained when the ray path within the resonance layer is longest. The strong sensitivity of the absorption to the launching geometry is experimentally studied with a top launch injected power as high as 0.9 MW in a variety of plasma configurations and comparisons between the experimental results with predictions from the ray tracing/absorption code TORAY-GA are presented.

Experimental results and Discussion

A preliminary study performed by Hogge et al. [1] was mainly dedicated to the commissioning of the X3 system and in particular to the steering capabilities of the top-launcher together with a study of the sensitivity of the plasma response to the launcher injection angle. In the same configuration for the X3 system as reported in [1], with 2 X3 gyrotrons connected to the top-launcher and 1 X3 gyrotron connected to a X2-Low Field Side launcher, it has been demonstrated that the ray-tracing/absorption code TORAY-GA gives accurate predictions of the absorbed power at moderate densities ($< 5 \cdot 10^{19} \text{ m}^{-3}$) and low temperatures ($< 1.5\text{-}1.7 \text{ keV}$). However, at larger densities, the agreement deteriorates and further study is required.

The experiments reported here were aimed at more detailed and quantitative studies of the ECRH capabilities of the X3 top-launch in terms of single-pass absorption in a variety of plasma conditions with plasma densities significantly higher than the X2 cutoff limit ($n_{\text{ecutoff}} = 4 \cdot 10^{19} \text{ m}^{-3}$). The target plasmas used in these experiments have the following parameters: major radius $R = 0.88\text{m}$; minor radius, $a = 0.25\text{m}$; toroidal magnetic field, $B_T = 1.45 \text{ T}$; elongation, $\kappa = 1.55$; triangularity, $\delta = 0.1\text{-}0.15$; peak electron densities ranging from 2 to $6 \cdot 10^{19} \text{ m}^{-3}$. The main diagnostics used are: the Thomson scattering for the measurement of both the bulk electron temperature and density (every 50ms), for suprathermal electrons the high field side ECE radiometer (ECE-HFS)[2] and for the evolution of the total plasma energy the

DML diagnostic[3]. The absorbed RF power, P_{in} , is measured during a modulated period of the X3 RF pulse using the diamagnetic loop[3, 4].

Two different scenarios were studied: the first with X3 top-launch heating only on an ohmic target plasma with density ranging from 2 to 6 10^{19} m^{-3} . The second scenario uses X2 central preheating at various power levels combined with X3 top-launch ECRH. In this scenario, the X2 aiming in pure ECRH does not produce a suprathermal tail during the X2 preheating phase and therefore allows the measurement of the X3 absorption on the bulk of the electron distribution. In an earlier study [5], with the X3 RF-power injected from the LFS in presence of a suprathermal tail generated by X2 CO-ECCD, it was shown that full single-pass X3 absorption was measured with approximately 50% absorbed on the bulk and 50% absorbed on the suprathermal tail generated by the X2 wave.

For the first scenario, the launching geometry as well as time traces of the relevant plasma parameters is shown in Fig.1.

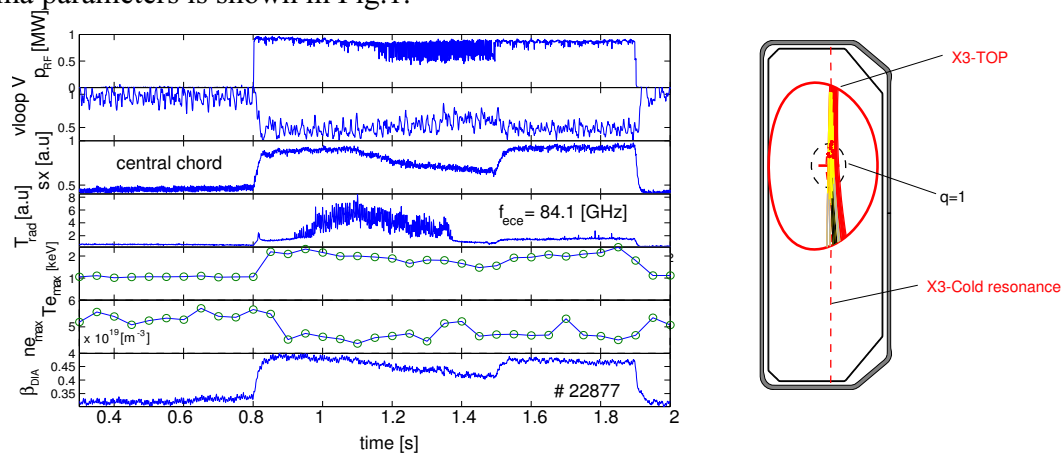


Figure 1. From top to bottom: RF power for X3 corresponding to 0.9 MW of injected power, loop voltage, soft X-ray signal (central chord), non-calibrated radiation temperature from one channel of the ECE-HFS radiometer, peak temperature and density from Thomson scattering (every 50ms) and diamagnetic β . Plasma current: $I_p = 230 \text{ kA}$. On the right part, the plasma cross-section with the ray-tracing calculated with the TORAY-GA code.

For this shot, the central electron density, $n_{e0} = 4.5\text{-}5 \cdot 10^{19} \text{ m}^{-3}$, is above the cutoff density for the X2 system ($4 \cdot 10^{19} \text{ m}^{-3}$) and the aiming of the top launcher mirror was kept fixed at an angle of 46.2 degrees (measured from the vertical clockwise). The optimum angle was determined in an earlier shot with same plasma parameters, but with an injection angle swept between 45.5 and 47.5 degrees. At $n_{e0} = 4.5 \cdot 10^{19} \text{ m}^{-3}$, the ECE-HFS radiometer channel is in cutoff and the observed deviation of the signal (0.9s – 1.3s) from its base level is to be associated with the presence of suprathermal electrons generated by the X3 wave. The fast electrons are spatially located outside the normalized radius of $r/a > 0.2$; the $q=1$ radius of this plasma is located at $r/a = 0.3$.

The absorption measurement with the DML is made during the RF power modulation of only one gyrotron (square wave at 237Hz) between $t = 1.2\text{s}$ and 1.4s . The measured absorbed power of the modulated gyrotron is $P_{abs} = 290\text{kW}$ which corresponds to an absorbed fraction of the X3 wave of 65%. Preliminary analysis shows that this value corresponds to single-pass absorption. When the top-launcher is swept during the shot over a wide angular range, whenever the aiming is far from the optimum angle, the main plasma parameters remain at the same level as without X3 power injection. As shown in Figure 2, with this launching geometry the deposition profile calculated with the TORAY-GA code gives a central deposition with the RF power deposited inside a normalized radius of $r/a = 0.45$ and an absorbed fraction of 32% which is significantly lower than the measured fraction of 66%.

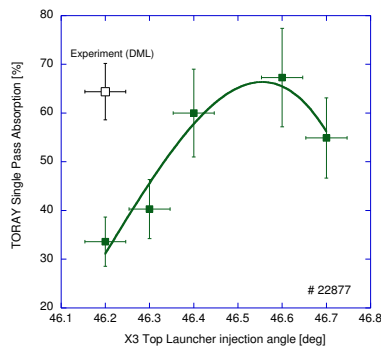


Figure 2. For this shot the X3 launch angle was fixed at 46.2° and the measured absorbed power was 66%. Using a launch angle of 46.2° TORAY-GA underestimates the absorbed power by 33%. By forcing TORAY-GA to use a launch angle of 46.55° agreement is obtained between the measured absorbed power and that predicted by TORAY-GA. Reasons for the discrepancy are being investigated. See main text for details.

The discrepancy between the two values might be explained by the sensitivity of the absorption on the launcher injection angle. By increasing the injection angle to 46.55° the deposition profile shape remains unchanged, but the total absorption predicted by the TORAY-GA code is significantly increased to 66%, in agreement with the measured value. The mechanical accuracy of the top-launcher mirror setting is better than 0.1° degrees and we believe that the discrepancy is to be found in the accuracy of the ray-tracing calculation on the reconstructed equilibrium. This effect, as well as other effects like beam diffraction (beam tracing [6]) or hot plasma effects on the refraction [7], are being investigated. In order to cope with the high sensitivity of the absorption on the launcher injection angle, plans to implement a real time feedback on the top-launcher mirror are underway. For the second scenario, which includes a X2 preheating phase (central with deposition within $r/a = 0.15$) before the turn on of the X3 wave, the launching geometry as well as time traces of the relevant plasma parameters are shown in Fig.3. In this shot the timing of the X2 (0.45 MW) is such that after the X2 turn-off (1.2s) the plasma density is increased from $2.2 \cdot 10^{19} \text{ m}^{-3}$ to $4.7 \cdot 10^{19} \text{ m}^{-3}$ within 500ms. The aiming of the top launcher mirror was kept fixed at an angle of 46.5 degrees. The predicted single-pass absorption by the TORAY-GA code depends, as expected, on the time evolution of the temperature and density profiles and ranges between a maximum of 85% at $t = 1.1\text{s}$ followed by a slight decrease at 71% to $t = 1.6\text{s}$ were X3 only is still on.

The stored energy variation, shown by the the diamagnetic signal (β_{DIA}), clearly shows that with 0.9 MW of RF power, the X3 top launch at high density ($4.5 \cdot 10^{19} \text{ m}^{-3}$) is able to maintain the same level of stored energy as for the combined X2-X3 phase with a significantly lower density ($2.2 \cdot 10^{19} \text{ m}^{-3}$). In this type of scenario with varying density, the absorption sensitivity on refraction could be optimized by a real-time feedback on the top-launcher mirror using for instance the diamagnetic signal.

As for the previous shot, during the combined X2-X3 phase the X3 RF beam generates a suprathermal population which subsequently decays, at X2 turn-off, to the thermal level on a fairly long time scale ($> 200\text{ms}$). In an experiment where the mirror is swept during the shot, with the absorption location moving from the X3 cold resonance toward the high field side, one observes that the X3 top-launch selectively couples to the electron energy. This can be extremely useful for suprathermal electron dynamics studies. This observation is illustrated in Figure 4 where the soft-x ray signal (sensitive to the bulk) and one channel of the ECE-HFS radiometer are plotted against the top-launch aiming angle.

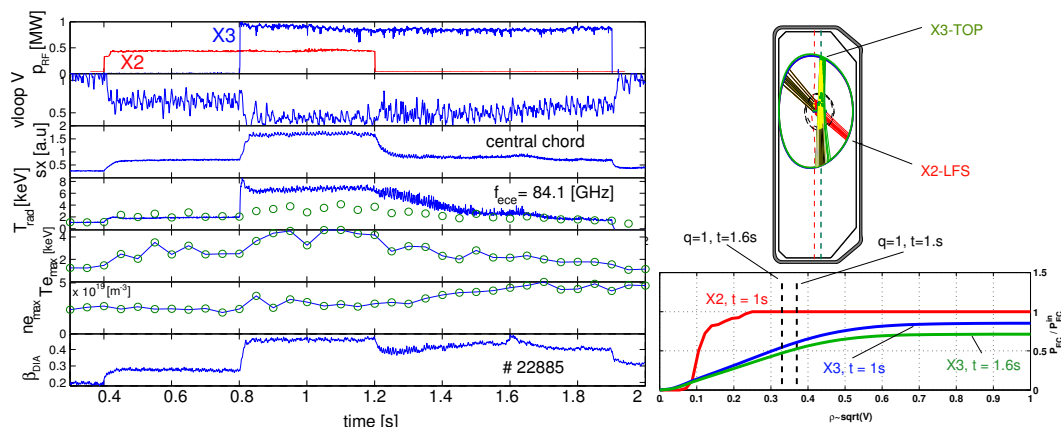


Figure 3. Same traces as in Figure 1 with in addition the calibrated radiation temperature (ECE-HFS) with the Thomson points at the corresponding radii of the ECE-channel. On the right part of the figure (top), the plasma cross section with the ray tracing for the X2 and X3 RF beams. On the right part of the figure (bottom), absorbed power versus normalized minor radius for the X2 beam (t=1s) and for the X3 beams at two different times (1s and 1.6s).

P-2.074

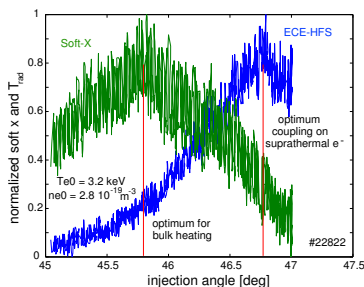


Figure 4. Presented here are a SXR signal (green) and an ECE signal (blue) from the same discharge plotted as a function of launcher angle. In this experiment the launcher angle is scanned. The SXR signal reflects heating on the bulk while the ECE signal reflects heating on the fast electron tail. As the mirror is scanned from the cold resonance to the high field side X3 power is selectively coupled to the bulk (SXR signal peak) and subsequently to the tail (ECE signal peak).

Conclusions

The X3 top-launch system significantly extends the operational regime of the TCV Tokamak. With X2 ECH preheating, single pass X3 absorptions as high as 90% have been measured. In a scenario where a density ramp is imposed after the X2 shutoff it is demonstrated that the stored plasma energy remains at the same level as for the X2 phase but with twice as high electron density. On a purely ohmic plasma at a density of $5.5 \cdot 10^{19} \text{ m}^{-3}$ a single-pass absorption as high as 66% has been measured. With the completion in the near future of the X3 top-launch system with 1.5MW of injected power, with higher electron temperatures, nearly full single-pass absorption is expected. Access to these higher density with additional heating will considerably extend the parameter range of confinement and transport already widely studied in TCV. The X3 top-launch flexibility has shown the possibility to selectively couple to different electron energies and could be used as a diagnostic for studies of the suprathermal electron dynamics.

References

- [1] J.-P. Hogge, S. Alberti, L. Porte, G.Arnoux, EC12
- [2] P. Blanchard, S. Alberti, S. Coda, H. Weisen, at this conference
- [3] G. Arnoux, A. Manini, S. Alberti, J.-M. Moret at this conference
- [4] A. Manini, et al., Plasma Phys. Control. Fusion (2002),
- [5] S. Alberti et al., Nucl. Fusion 42 (2002), 42.
- [6] S. Nowak and A.Orefice, Phys. Plasmas 1 (1994), 1242.
- [7] M.D. Tokman et al, EC12